

Statistical biases in measurements with multiple candidates

P. Koppenburg¹

¹*Nikhef, Amsterdam, Netherlands.*

Abstract

Many measurements at collider experiments study physics candidates that are a subset of a collision event. The presence of multiple such candidates in a given event can cause raw biases which are large compared to typical statistical uncertainties. Selecting a single candidate is common practice but only helps if the likelihood of selecting the true candidate is very high. Otherwise the precision of the measurement can be affected, and biases can be generated, even if none are present in the data sample prior to this operation.

This paper aims at describing the problem in a systematic way. It sets definitions, provides examples of potential biases using pseudoexperiments and gives recommendations.

This is the 2019 update of the original 2017 preprint.

Contents

1	Introduction	1
2	Definitions	2
2.1	Techniques	2
3	Pseudoexperiment	3
3.1	Varying companion probabilities	6
3.2	Arbitration	7
3.3	Flavour swaps	9
3.4	Continuous observables: lifetime and mass measurements	9
3.5	Efficiency corrections	11
4	Recommendations	12
5	Conclusion	13
	References	14

1 Introduction

In absence of new elementary particles produced in high-energy collisions, precision measurements provide the best way of finding signs of New Physics at colliders. These measurements require large data samples as well as a very detailed understanding of potential biases. As luminosities increase, much larger data samples are anticipated in the near future, notably at the Large Hadron Collider (LHC) or the KEKB e^+e^- collider. Many decay-rate or asymmetry measurements with a precision of order 10^{-4} are or will soon be available in flavour [1–3] physics, while electroweak and Higgs physics also enter the precision regime [4, 5]. The presence and the handling of multiple candidates per event can cause raw biases which may be large compared to anticipated accuracies. These biases can be corrected for, provided a proper strategy is employed, with some loss in precision.

In the following, *event* stands for all signals originating from a collision process, or a set of simultaneous processes, as in a single beam-bunch crossing. A *candidate* is the reconstructed particle of interest, including its decay chain, on which the measurement is being performed — typically a Higgs or Z boson, a top quark, or a B meson. The latter example is used below, as flavour physics is presently most affected by the effects described here.

The processes most commonly studied in modern high-energy physics have a small probability, either because the production rate is small (as for the Higgs boson [6, 7]) or because the decay rate is low (as for the decay $B_s^0 \rightarrow \mu^+\mu^-$ [8, 9]), or both. (Studies of processes that are not rare, and where several candidates per event are to be expected, are not in the scope of this paper.) The same applies to background, as analysts invest considerable effort to achieve a background rate of the same order as that of the signal, or less. Yet many high-energy physics analyses are affected by a nonnegligible fraction of events containing several candidates, typically in the range 0.1 to 20%. The probabilities of selecting one or a second candidate in an event are not uncorrelated. If they were — given the low probability involved — the rate of events containing two or more candidates would be vanishingly small. The presence of multiple candidates in an event is therefore an indication that the event or the candidates are atypical. An investigation is required prior to any action being taken.

Multiple-candidate events are a nuisance for the analysis. They contribute to the background level and thus degrade the sensitivity of the measurement. Most importantly, additional candidates can cause biases if their rate is correlated with the observable to be measured. These biases may be corrected using simulation or control samples, provided these are good representations of the data. Otherwise, additional corrections are required. Such situations are discussed in Sec. 3.

In some publications the rate of multiple candidates and the procedure to handle them is described, but less frequently are their origin discussed and potential biases addressed. It is usually not possible for the reader to assess their nature and their effect on the measurement, which affects the reproducibility of the analysis. No standard procedure to address multiple candidates is publicly documented (see Note [10]), which forces every collaboration or analysis group to decide how to address the problem (or to ignore it), and often to re-invent the wheel. Procedures applied in previous publications tend to be replicated without thinking about potential bias and loss of sensitivity. While the effects described here are small, their magnitude may be similar to the precision of

the measurement.

The present paper is an attempt at describing the problem in a systematic way. It is based on recommendations internal to the LHCb collaboration and is organised as follows: Sec. 2 gives definitions of sources of multiple candidates and techniques to address them. A set of pseudoexperiments assessing the size of potential biases is described in Sec. 3. Recommendations are given in Sec. 4.

2 Definitions

Multiple candidates can be of several kinds, listed below.

Overlaps share some of their reconstructed objects (tracks, clusters, jets. . .). If the signals are fully reconstructed, at most one of the overlapping candidates can be signal.

Reflections are candidates which share all reconstructed objects but with different particle-identification assignments. Depending on the analysis they can be peaking in mass (when applicable) or not. Their treatment is analysis dependent and thus not discussed further in this paper.

Genuine multiples do not share any of their properties. They could in principle be both signal, depending on the signal rate and selection efficiency [11], but are more likely to be both background (*e.g.* caused by a high-multiplicity event) or one of each.

Reconstruction features may make physics objects appear multiple times. They are experiment specific and therefore their effect on the measurement is not discussed here. However, they need to be considered when dealing with multiple candidates.

2.1 Techniques

Several techniques of handling multiple candidates are reported in the literature.

No action: The simplest and most frequent approach is to take *no action*, i.e. keep all candidates for further analysis. The reader has to assume that this was the chosen approach when multiple candidates are not mentioned in a publication [13]. In some publications this choice is explicitly mentioned [14–30]. It is the correct approach in production cross-section measurements [31–40].

Sample splitting: In rare occasions, the data sample is *split* by candidate multiplicity [41]. A different background parametrisation depending on the presence of multiple candidates is then used.

All other techniques aim at reducing the level of multiple candidates.

Arbitration consists in attempting to identify the true signal candidate by using a discriminating variable, thus applying a tighter selection in events with multiple candidates compared to the remaining events. Typical choices of variables are the (transverse [42, 43]) momentum [44] of the candidate or of a decay product, the

χ^2 of a vertex [45–49] or of a decay tree fit [50–52], an impact parameter [53, 54], a flight length [55], a mass of a decay product [6, 56–62], the particle-identification likelihood of a final-state particle [63], the output of a multivariate classifier [64], the expected rate of the final state [61], or, the beam-constrained energy at e^+e^- colliders [65–71]. Arbitration may also be part of the event reconstruction [72] and the selection of the collision point [73].

Random picking is a special case of arbitration where the chosen variable is a random number and thus not discriminating [1, 74–92]. A variant of random picking is *weighting*, in which candidates are weighted by the inverse of their multiplicity [93].

Event removal, where all events with multiple candidates are discarded, is also occasionally used [94–98].

The above-mentioned techniques have an associated signal efficiency, which contributes to the total selection efficiency. The latter is often determined using simulated data or a control channel, which may incorrectly model the candidate multiplicity. This is discussed further in Sec 3.5.

3 Pseudoexperiment

The effect of the candidate multiplicity is tested with a set of pseudoexperiments. The model employed here is typical of a B physics experiment, but is kept intentionally simple, so that it can be translated to any scenario. The only needed features are that the signal is separated from the background by a fit to a discriminating variable (here a mass). The properties of the signal are then investigated.

The problem is formulated as follows. A process resulting in a Gaussian-shaped signal peak (a B^0 meson mass in this example) is studied. The rate (which could result in the measurement of a cross-section or a branching fraction), an asymmetry, and a property (here the lifetime) are to be measured. Ratios and asymmetries are of particular interest as many of the detector- and selection-related biases cancel at first order. They allow for high-precision measurements which can be compared with precise predictions. Here a CP or production asymmetry between the B^0 and \bar{B}^0 yields is taken as an example, but the problem can be generalised to any fraction, as for instance a polarisation.

In the present example $N_{B^0}^{\text{orig}} = 50\,000$ signal B^0 mesons are generated (including Poisson fluctuations) on top of as many combinatorial background candidates. The B^0 signal is represented by a Gaussian shape and the background has a uniform mass distribution [99] in a range of 25 times the resolution and is centred on the signal. The same is done for \bar{B}^0 mesons. This starting point, before additional candidates are added, is referred to as the *clean* case and the initial candidates are called *original*.

Next, additional candidates (called *companions*) are generated as follows.

1. Each signal B^0 meson has a probability $\mathcal{P}_{\text{sig}}^{B^0}$ to have a companion candidate in the same event. The mass distribution of these candidates is background-like [100]. This candidate can have a swapped flavour [101], with probability $\mathcal{P}_{\text{swap}}^{\text{sig } B^0}$, or have the same flavour, with probability $(1 - \mathcal{P}_{\text{swap}}^{\text{sig } B^0})$.

2. The same is done for \bar{B}^0 mesons, introducing the probabilities $\mathcal{P}_{\text{sig}}^{\bar{B}^0}$ and $\mathcal{P}_{\text{swap}}^{\text{sig } \bar{B}^0}$, which do not need to be identical to those for B^0 mesons.
3. Each background B^0 candidate has a probability $\mathcal{P}_{\text{bkg}}^{B^0}$ to have a companion candidate with probability of swapped flavour $\mathcal{P}_{\text{swap}}^{\text{bkg } B^0}$, generated with uniform mass.
4. The same is done for \bar{B}^0 background candidates with probabilities $\mathcal{P}_{\text{bkg}}^{\bar{B}^0}$ and $\mathcal{P}_{\text{swap}}^{\text{bkg } \bar{B}^0}$, which do not need to be identical to those for B^0 background candidates.

All symbols defined above are listed in Table 1, along with symbols defined later in this section.

In absence of flavour swaps, the fraction of events with multiple candidates is given

Table 1: Symbols used in this document.

Symbol	Definition
$N_{B^0}^{\text{orig}}$	Original number of signal B^0 mesons (= 50 000)
$N_{\bar{B}^0}^{\text{orig}}$	Original number of signal \bar{B}^0 mesons (= 50 000)
$N_{\text{bkg } B^0}^{\text{orig}}$	Original number of background B^0 mesons (= 50 000)
$N_{\text{bkg } \bar{B}^0}^{\text{orig}}$	Original number of background \bar{B}^0 mesons (= 50 000)
$N_{B^0}^{\text{bkg}}$	Total number of background B^0 candidates
$N_{\bar{B}^0}^{\text{bkg}}$	Total number of background \bar{B}^0 candidates
τ_{B^0}	B^0 meson lifetime (= 1.52 ps)
α	Inverse effective signal-to-background ratio
$N_{B^0}^{\text{fit}}$	Measured B^0 signal yield
$N_{\bar{B}^0}^{\text{fit}}$	Measured \bar{B}^0 signal yield
A_{raw}	Asymmetry between measured B^0 and \bar{B}^0 signal yields
$\mathcal{P}_{\text{sig}}^{B^0}$	Probability of a B^0 meson to have a companion in the event
$\mathcal{P}_{\text{sig}}^{\bar{B}^0}$	Probability of a \bar{B}^0 meson to have a companion in the event
$\mathcal{P}_{\text{bkg}}^{B^0}$	Probability of a background B^0 candidate to have a companion in the event
$\mathcal{P}_{\text{bkg}}^{\bar{B}^0}$	Probability of a background \bar{B}^0 candidate to have a companion in the event
R_{all}	Fraction of events with multiple candidates
R_{B^0}	Fraction of signal events with multiple candidates
$\mathcal{P}_{\text{swap}}^{\text{sig } B^0}$	Probability of a signal B^0 companion to have a \bar{B}^0 flavour
$\mathcal{P}_{\text{swap}}^{\text{sig } \bar{B}^0}$	Probability of a signal \bar{B}^0 companion to have a B^0 flavour
$\mathcal{P}_{\text{swap}}^{\text{bkg } B^0}$	Probability of a background B^0 companion to have a \bar{B}^0 flavour
$\mathcal{P}_{\text{swap}}^{\text{bkg } \bar{B}^0}$	Probability of a background \bar{B}^0 companion to have a B^0 flavour
$\eta_{\text{best}}^{B^0}$	Efficiency of picking the signal B^0 when the companion has the same flavour
$\eta_{\text{best}}^{\bar{B}^0}$	Efficiency of picking the signal \bar{B}^0 when the companion has the same flavour
$\eta_{\text{best}}^{B^0/\bar{B}^0}$	Efficiency of picking the signal B^0 when the companion has a different flavour
$\eta_{\text{best}}^{\bar{B}^0/B^0}$	Efficiency of picking the signal \bar{B}^0 when the companion has a different flavour

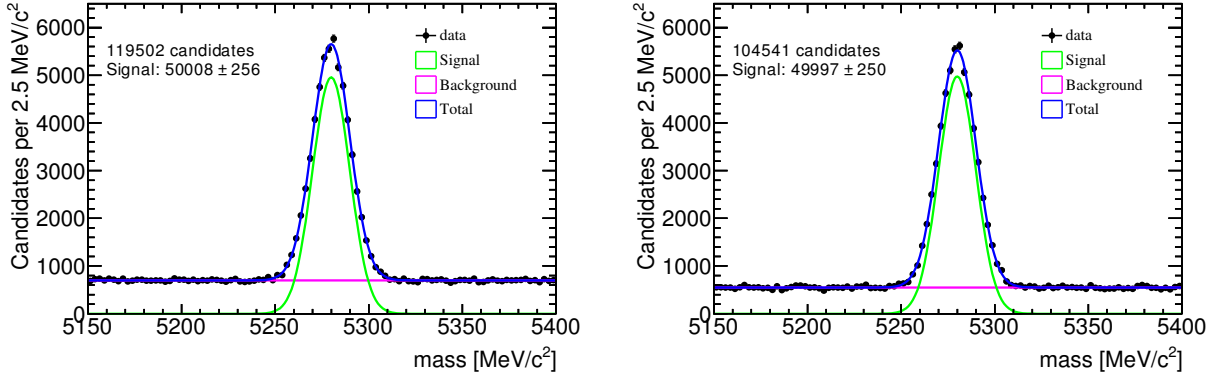


Figure 1: Typical mass distributions after companion addition for (left) B^0 and (right) \bar{B}^0 candidates with $\mathcal{P}_{\text{sig}}^{B^0} = 0.4$, $\mathcal{P}_{\text{sig}}^{\bar{B}^0} = 0.1$. All other probabilities of Table 1 are set to zero. The number of candidates and the fitted signal yield are indicated.

by

$$R_{\text{all}} = \frac{\mathcal{P}_{\text{sig}}^{B^0} N_{B^0}^{\text{orig}} + \mathcal{P}_{\text{bkg}}^{B^0} N_{\text{bkg } B^0}^{\text{orig}}}{N_{B^0}^{\text{orig}} + N_{\text{bkg } B^0}^{\text{orig}}}. \quad (1)$$

The analogous quantity can be defined *mutatis mutandis* for \bar{B}^0 mesons but is not used in the following. This emulation is a simplified model of reality as there are no events with three candidates. As all candidates have passed all selection requirements, they are equally signal-like except for their mass.

After the addition of companions, the B^0 and \bar{B}^0 background levels are increased by amounts depending on the values of the above-defined probabilities. Typical mass distributions are shown in Fig. 1 for $\mathcal{P}_{\text{sig}}^{B^0} = 0.4$ and $\mathcal{P}_{\text{sig}}^{\bar{B}^0} = 0.1$. Here and in the following, large probabilities are used to make the effects easily visible in graphics. In a real experiment, the probabilities would be smaller, but the total yields may be much larger, making the described effects significant.

Taking no action results in keeping all candidates, and is referred to as the *all* scenario. Alternatively, the analyst can choose to pick a *random* candidate or perform an *arbitration*. Weighting and event removal are not tested. Their effect can be inferred from those of the random selection [102]. After this operation the B^0 and \bar{B}^0 yields are determined separately from unbinned maximum-likelihood fits to the mass distributions. The probability distribution function used in the fit is the sum of a Gaussian and a uniform background; the same as is used in the generation of the sample. All parameters are left free in the fit.

The uncertainty on the signal yield $N_{B^0}^{\text{fit}}$ depends on the background yield $N_{B^0}^{\text{bkg}}$ as

$$\sigma(N_{B^0}^{\text{fit}}) = \sqrt{N_{B^0}^{\text{fit}} + \alpha N_{B^0}^{\text{bkg}}}, \quad (2)$$

where to a good level of approximation α only depends on the mass window and the signal peak resolution. In this case $\sigma(N_{B^0}^{\text{fit}}) = 248$ and $\alpha = 0.23$. The example in Fig. 1 shows that while the probabilities of companion candidates are different, resulting in a higher background level for B^0 candidates, the fits return signal yields consistent with the generated multiplicity. As expected, the uncertainty is larger in the case of a higher candidate multiplicity.

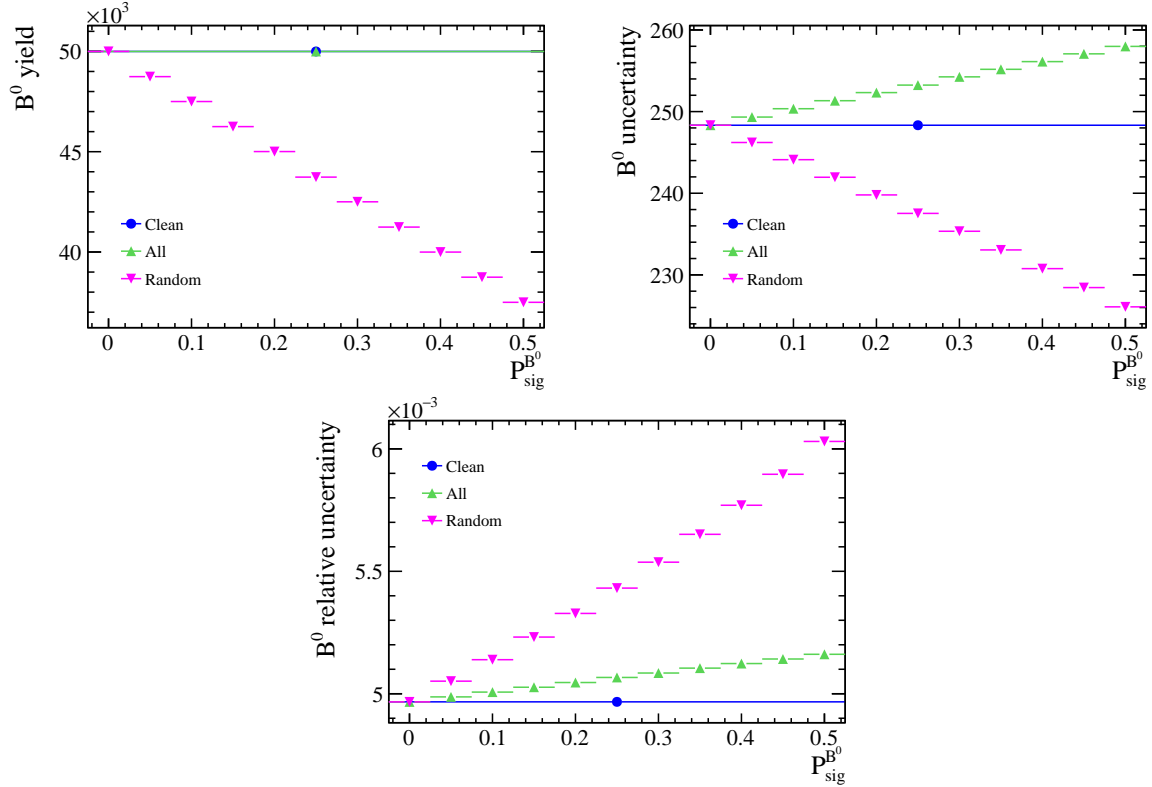


Figure 2: Measured B^0 (top left) yield, (top right) uncertainty and (bottom) their ratio versus $\mathcal{P}_{\text{sig}}^{B^0}$. All other probabilities of Table 1 are set to zero. Beware that all plots have a zero-suppressed vertical axis. The yields vary linearly with the probabilities while the uncertainties follow a square-root law, which is almost linear on this scale.

Multiple-candidate handling techniques are studied as function of the probabilities defined above with thousand pseudoexperiments per set of probabilities. The results shown below are averages on these pseudoexperiments. Many of the subsequent results can be determined analytically using the probabilities listed in Table 1 and behave almost linearly with the input probabilities [103].

3.1 Varying B^0 companion probabilities

First the signal probabilities $\mathcal{P}_{\text{sig}}^{B^0}$ and $\mathcal{P}_{\text{sig}}^{B^0}$ are varied between 0 and 0.5 with $\mathcal{P}_{\text{bkg}}^{B^0} = \mathcal{P}_{\text{bkg}}^{B^0} = 0$. The resulting measured B^0 yields and uncertainties are reported in Figure 2.

The ideal clean case, in which always the correct candidate is picked, is the benchmark scenario with which all other approaches are compared. When using all candidates the correct yield is obtained, although with an increased uncertainty. With the technique consisting of randomly picking candidates, the signal candidate is discarded in half of the events with multiple candidates. The fit returns a biased B^0 yield, trivially depending on $\mathcal{P}_{\text{sig}}^{B^0}$ as

$$(N_{B^0}^{\text{fit}})^{\text{random}} = N_{B^0}^{\text{orig}} \left(1 - \frac{1}{2} \mathcal{P}_{\text{sig}}^{B^0} \right). \quad (3)$$

The biases can be corrected (see Section 3.5), but not the loss of statistical precision.

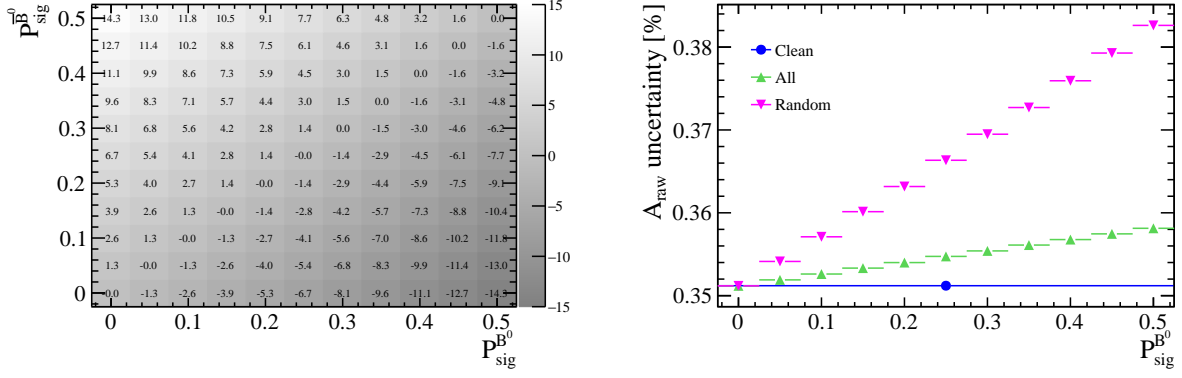


Figure 3: (left) Measured A_{raw} (in percent) versus $\mathcal{P}_{\text{sig}}^{B^0}$ and $\mathcal{P}_{\text{sig}}^{\bar{B}^0}$ for random picking. (right) Uncertainty on this quantity for the three techniques versus $\mathcal{P}_{\text{sig}}^{B^0}$, with $\mathcal{P}_{\text{sig}}^{\bar{B}^0} = 0$. All other probabilities of Table 1 are set to zero.

The relative uncertainty on the B^0 yield [103] — which is often the quantity for which the selection is optimised — is shown in Fig. 2 (bottom). The random selection technique performs worse than taking all with respect to this figure of merit.

Next, an asymmetry between the B^0 and \bar{B}^0 yields is determined, defined by

$$A_{\text{raw}} = \frac{N_{B^0}^{\text{fit}} - N_{\bar{B}^0}^{\text{fit}}}{N_{B^0}^{\text{fit}} + N_{\bar{B}^0}^{\text{fit}}}. \quad (4)$$

In the following pseudoexperiments no asymmetry is generated and any measurement of this quantity should be consistent with zero. Figure 3 show this asymmetry versus the $\mathcal{P}_{\text{sig}}^{B^0}$ and $\mathcal{P}_{\text{sig}}^{\bar{B}^0}$ probabilities in the range 0 to 0.5. Asymmetries of up to 14% can be generated when performing random picking. Using Eq. 3, the expected asymmetry is easily calculable as

$$(A_{\text{raw}})_{\text{random}} = \frac{N_{B^0}^{\text{orig}} \left(1 - \frac{1}{2} \mathcal{P}_{\text{sig}}^{B^0}\right) - N_{\bar{B}^0}^{\text{orig}} \left(1 - \frac{1}{2} \mathcal{P}_{\text{sig}}^{\bar{B}^0}\right)}{N_{B^0}^{\text{orig}} \left(1 - \frac{1}{2} \mathcal{P}_{\text{sig}}^{B^0}\right) + N_{\bar{B}^0}^{\text{orig}} \left(1 - \frac{1}{2} \mathcal{P}_{\text{sig}}^{\bar{B}^0}\right)} \underset{A_{CP}=0}{=} \frac{\mathcal{P}_{\text{sig}}^{\bar{B}^0} - \mathcal{P}_{\text{sig}}^{B^0}}{4 - \mathcal{P}_{\text{sig}}^{B^0} - \mathcal{P}_{\text{sig}}^{\bar{B}^0}}, \quad (5)$$

where the expression considerably simplifies when no true CP asymmetry is present. On the other hand, using all candidates leaves the asymmetry unbiased.

The uncertainties on this quantity vary from 0.362%, at $\mathcal{P}_{\text{sig}}^{B^0} = \mathcal{P}_{\text{sig}}^{\bar{B}^0} = 0$, to values of 0.366% for random picking and 0.382% when keeping all candidates. These changes in statistical uncertainties are very small (+0.02%) in comparison with the potential bias introduced by the random picking technique (up to 14%). Similarly, varying the companion probabilities in background, $\mathcal{P}_{\text{bkg}}^{B^0}$ and $\mathcal{P}_{\text{bkg}}^{\bar{B}^0}$, only slightly affects the statistical uncertainties [104].

3.2 Arbitration

The drawbacks of random picking may be cured by arbitration. The selection of a “best” candidate is done using an observable O which is not correlated to that which is used to

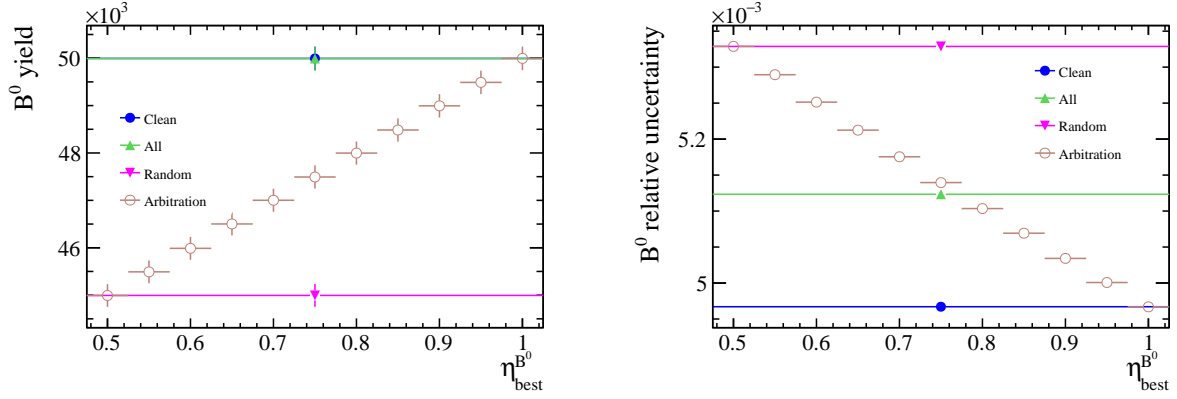


Figure 4: (left) B^0 yield and (right) relative uncertainty versus efficiency of picking the signal candidate $\eta_{best}^{B^0}$. The value at $\eta_{best}^{B^0} = 0.5$ corresponds to random picking. The other parameters are set to $\mathcal{P}_{sig}^{B^0} = \mathcal{P}_{bkg}^{B^0} = 0.2$, $\mathcal{P}_{swap}^{sig B^0} = \mathcal{P}_{swap}^{bkg B^0} = 0$.

determine the signal yield (here the candidate mass). For the technique to be effective, the true signal and the other candidates must have different distributions of this quantity. This feature is exploited to pick the candidate that is most signal-like. The arbitration procedure has an efficiency $\eta_{best}^{B^0}$ of picking the true signal, which should be as high as possible. For the present discussion, only this efficiency matters, and not the actual O distributions.

The aim is illustrated in Figure 4 (left). As the efficiency of picking the right candidate is improved, the measured B^0 yield increases linearly from the value obtained with random picking to that of a perfect selection. The biases caused by random picking (Eq. 3) are mitigated by arbitration as $\eta_{best}^{B^0}$ approaches unity,

$$(N_{B^0}^{fit})^{arbitration} = N_{B^0}^{orig} \left(1 - \eta_{best}^{B^0} \mathcal{P}_{sig}^{B^0}\right). \quad (6)$$

Similarly, the effect of the arbitration procedure on the biases of A_{raw} can be obtained by multiplying the values of Figure 3 (left) by $2(1 - \eta_{best}^{B^0})$.

With increasing values of $\eta_{best}^{B^0}$, the relative uncertainty on the B^0 yield decreases and becomes better than that obtained using all candidates. The value of the crossing point in Fig. 4 (right) depends on $\eta_{best}^{B^0}$, $\mathcal{P}_{sig}^{B^0}$ and $\mathcal{P}_{bkg}^{B^0}$ [103]. It is to be noted again that the relative uncertainty varies very little. As for random picking, the gain in statistical sensitivity is small compared to the potential biases due to potentially different values of $\mathcal{P}_{sig}^{B^0}$ and $\mathcal{P}_{sig}^{\bar{B}^0}$.

A best-candidate selection only helps if the efficiency for selecting the correct candidate is very large. Otherwise, additional asymmetries can be generated, even if none are present in the data prior to this operation. The best candidate selection efficiency can be different for B^0 and \bar{B}^0 mesons, $\eta_{best}^{\bar{B}^0} \neq \eta_{best}^{B^0}$, if the distributions of the O observable are different for B^0 and \bar{B}^0 signal, background, or both. Such an asymmetry of selection efficiencies can induce biases of the B^0 and \bar{B}^0 yields, generating raw asymmetries, as shown in Figure 5. In the (unlikely) extreme cases, raw asymmetries of 5% can be reached.

In a real measurement, analysts would not pick an observable which can generate large asymmetries. However, even if checked, this fact is hardly ever reported in

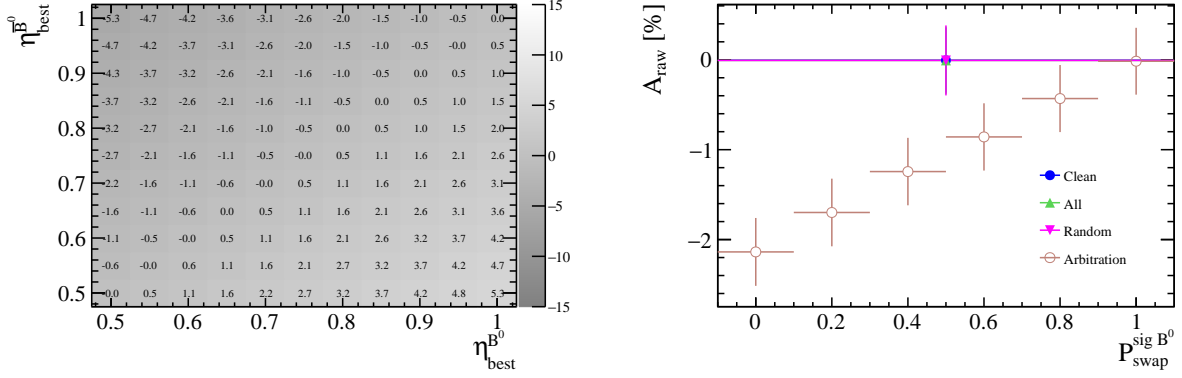


Figure 5: A_{raw} (in percent) versus (left) efficiencies of picking the signal candidate $\eta_{\text{best}}^{B^0}$ and $\eta_{\text{best}}^{\bar{B}^0}$, and (right) versus flavour swapping probability $\mathcal{P}_{\text{swap}}^{\text{sig } B^0}$. Other parameters are set to $\mathcal{P}_{\text{sig}}^{B^0} = \mathcal{P}_{\text{sig}}^{\bar{B}^0} = \mathcal{P}_{\text{bkg}}^{B^0} = \mathcal{P}_{\text{bkg}}^{\bar{B}^0} = 0.2$. Additionally in the right plot, $\eta_{\text{best}}^{B^0} = \eta_{\text{best}}^{\bar{B}^0/B^0} = 0.6$, $\eta_{\text{best}}^{\bar{B}^0} = \eta_{\text{best}}^{B^0/\bar{B}^0} = 0.8$ and $\mathcal{P}_{\text{swap}}^{\text{sig } \bar{B}^0} = \mathcal{P}_{\text{swap}}^{\text{bkg } B^0} = 0$. $\mathcal{P}_{\text{swap}}^{\text{sig } B^0} = \mathcal{P}_{\text{swap}}^{\text{bkg } \bar{B}^0}$ is imposed. The vertical error bars represent the average uncertainty on the fitted asymmetry.

publications. Also, the asymmetry of the observable is only known to a given precision, which in principle should be determined and assigned as a systematic uncertainty [105].

3.3 Flavour swaps

In the above, it is assumed that all companions have the same flavour as the original candidate, or that it is irrelevant. This is not necessarily the case. For overlapping candidates, the flavour of the signal B meson and that of the other candidate may be correlated, or anti-correlated [106]. The consequence are non-identical probabilities of being accompanied by a candidate of different flavour $\mathcal{P}_{\text{swap}}^{\text{sig } B^0}$, $\mathcal{P}_{\text{swap}}^{\text{sig } \bar{B}^0}$ for B^0 and \bar{B}^0 signal, and $\mathcal{P}_{\text{swap}}^{\text{bkg } B^0}$, $\mathcal{P}_{\text{swap}}^{\text{bkg } \bar{B}^0}$ for B^0 and \bar{B}^0 background.

In Figure 5 (right) the swapping probabilities $\mathcal{P}_{\text{swap}}^{\text{sig } B^0}$ and $\mathcal{P}_{\text{swap}}^{\text{sig } \bar{B}^0}$ are varied (synchronously with $\mathcal{P}_{\text{swap}}^{\text{bkg } B^0}$ and $\mathcal{P}_{\text{swap}}^{\text{bkg } \bar{B}^0}$, which have no effect), for $\eta_{\text{best}}^{B^0} = 0.6$ and $\eta_{\text{best}}^{\bar{B}^0} = 0.8$. Values of -2.1% for A_{raw} are obtained when the swapping probabilities are identical. This corresponds to the point at $\eta_{\text{best}}^{B^0} = 0.6$, $\eta_{\text{best}}^{\bar{B}^0} = 0.8$ in Fig. 5 (left). Different swapping probabilities can mitigate the problem up to hiding it completely, as for the extreme case $\mathcal{P}_{\text{swap}}^{\text{sig } B^0} = 1$ [107].

3.4 Continuous observables: lifetime and mass measurements

Next, the data described above is used to measure the lifetime of B^0 mesons. It is assumed that the decay-time distributions of the signal and background follow a falling exponential of constants $-\tau_{B^0}$ and $-\tau_{B^0}/3$, respectively. For companion candidates overlapping with the signal this constant is taken to be $-\tau_{B^0}/2$ [108].

The three exponential distributions are convolved with a Gaussian-shaped resolution function [109]. No time-dependent selection effects are considered. This situation leads to a distribution as shown in Fig. 6 (left), where the three contributions are shown.

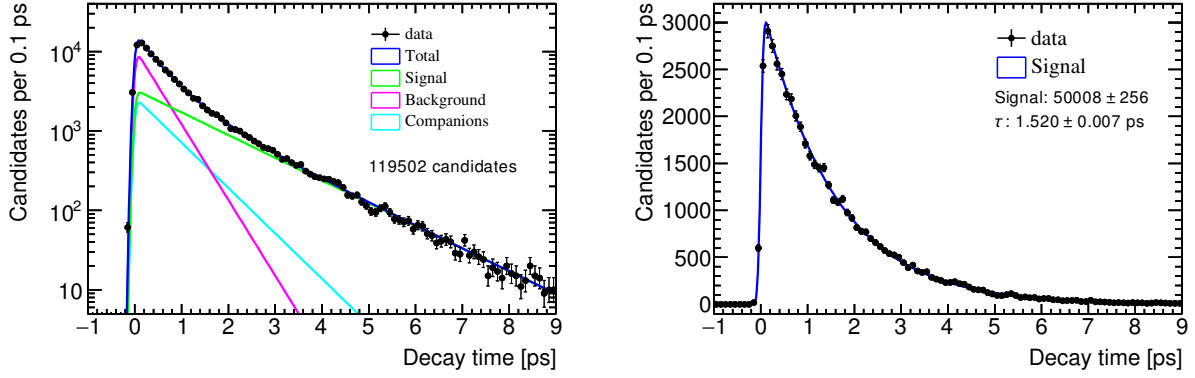


Figure 6: Typical decay-time distribution after companion addition for (left) all candidates and (right) background-subtracted signal. As in Fig. 1 (left), the companion probability is $\mathcal{P}_{\text{sig}}^{B^0} = 0.4$. All other probabilities of Table 1 are set to zero.

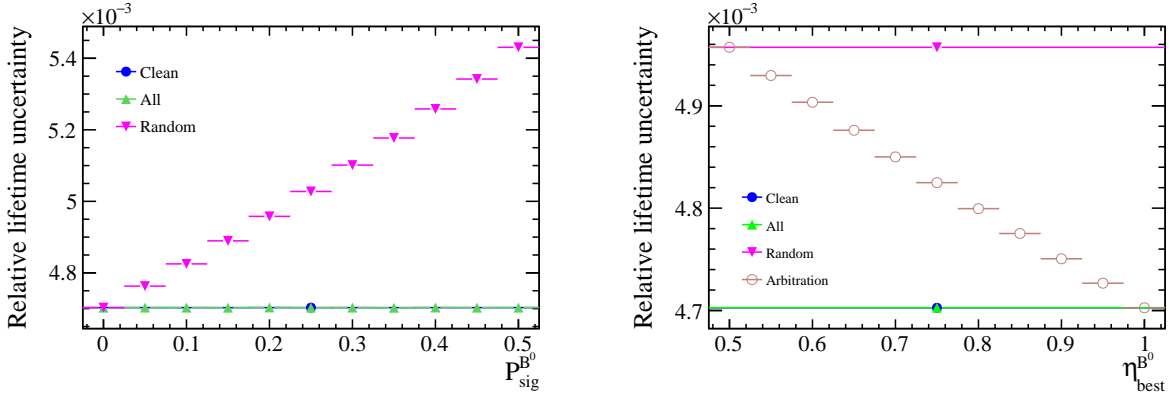


Figure 7: Relative uncertainty on lifetime versus (left) $\mathcal{P}_{\text{sig}}^{B^0}$ and (right) $\eta_{\text{best}}^{B^0}$. All other probabilities are set to zero in the former case, while $\mathcal{P}_{\text{sig}}^{B^0} = \mathcal{P}_{\text{bkg}}^{B^0} = 0.2$ in the latter case.

If the mass and decay time are not correlated for the three above-defined species, the *sPlot* technique [110, 111] can be used to statistically subtract the background and companion candidates using their distinct mass distributions. The decay-time distribution for signal is thus obtained with an unbinned maximum-likelihood fit of a single exponential to the background-subtracted data, as shown in Fig. 6 (right). As companion candidates do not peak in mass they do not affect the signal decay-time distribution and no biases can be caused [112]. The additional background causes an increased relative uncertainty on the fitted lifetime value, as shown in Fig. 7. Taking all candidates does not bias the measurement, and has a negligible effect on the uncertainty. Random picking and arbitration degrade the resolution due to the loss of signal.

The lifetime can also be determined by fitting all data with a signal and one or several background components [113]. If the specific features of overlapping companions are ignored, only one component for the background is used. Such a fit is shown in Fig. 8 (left). The measured lifetime is biased, as seen in Fig. 8 (right). For large data samples, the missing component would lead to poor fits, as in this example. However, it could easily be missed in case of smaller samples. Sums of similar exponential distributions

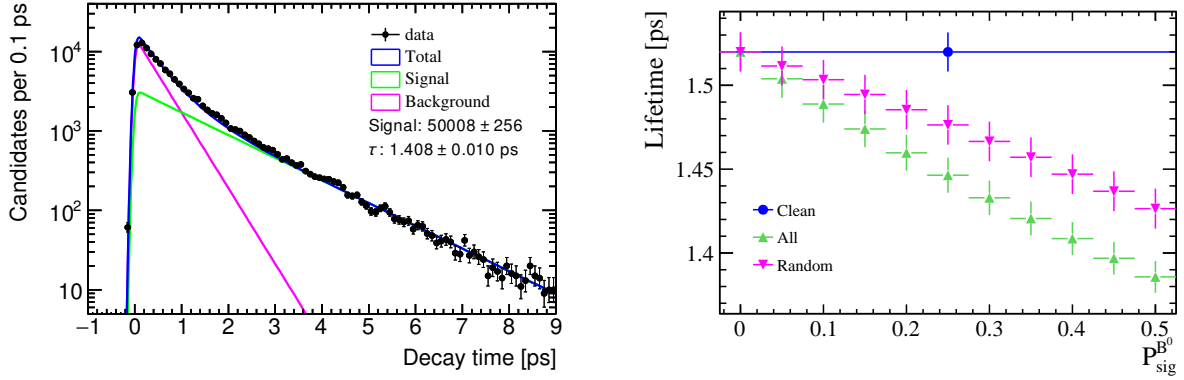


Figure 8: (left) Two-component fit to the lifetime data which was generated with three exponential functions. The companion probability is $\mathcal{P}_{\text{sig}}^{B^0} = 0.4$. All other probabilities of Table 1 are set to zero. (right) Measured lifetime versus $\mathcal{P}_{\text{sig}}^{B^0}$. The vertical error bars represent the average uncertainty on the fitted lifetime.

can be well fitted by a single exponential [114], resulting in biased lifetime results.

This issue is cured by the use of the *sPlot* technique, as shown above. But this technique does not apply to quantities which are correlated with the discriminating variable. For instance the measurement of the mass of a resonance requires a good understanding of the background shape. If overlapping companions tend to accumulate at masses close to but, somewhat lower than, the signal, the fit could return a biased value [60, 61, 115, 116].

3.5 Efficiency corrections

Biases can be caused by the presence of companion candidates, or by the technique used to remove them. These biases can in principle be corrected for, but this correction requires a good knowledge of their sizes. The efficiency of the arbitration technique is $1 - (1 - \eta_{\text{best}}^{B^0})R_{\text{all}}$, where the fraction of events with multiple candidates R_{all} is given in Eq. 1. For a random selection $\eta_{\text{best}}^{B^0} = 1/2$. The fraction R_{all} is often reported in publications, giving the reader an estimate of the scale of the problem. For a quantitative estimate of the effect of the multiple-candidate handling procedure, $\eta_{\text{best}}^{B^0}$ is needed, as well as the fraction of signal events with multiple candidates, R_{B^0} (defined in analogy with R_{all} , setting $N_{\text{bkg } B^0}^{\text{orig}} = 0$ in Eq. 1). Only rarely are both numbers given.

Simulated signal events can be used to determine these numbers, provided that the simulation properly describes the companion candidate rate and distribution. At B or charm factories, where the underlying event is the other heavy meson [70, 71], the simulation is often reported to correctly model multiple candidates. The description of the underlying event at hadron colliders is less reliable [117, 118]. The analyst may have to deal with a different fraction and composition of companion candidates in the simulation and the data. Different candidate removal efficiencies in data and simulation lead to a potentially large systematic uncertainty, which is rarely reported in publications. This uncertainty depends on the properties of the underlying event, while prior to candidate removal only the signal efficiency is relevant.

The efficiency can also be assessed using data, for instance applying the *sPlot*

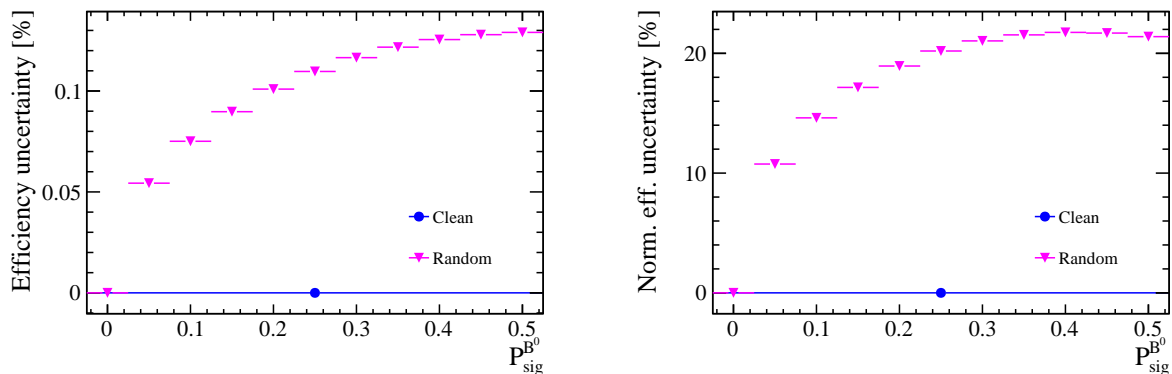


Figure 9: (left) Uncertainty on the efficiency of randomly picking the true signal B versus $\mathcal{P}_{\text{sig}}^{B^0}$. (right) Ratio of this uncertainty to the relative uncertainty on the signal yield (Fig. 2, bottom). All other probabilities of Table 1 are set to zero.

technique used in Sec. 3.4, or similar background-subtraction techniques. In the present set of pseudoexperiments, the efficiency of random picking is determined without bias [119] from the candidate multiplicity in events with signal. The uncertainty on this efficiency is in the per-mille range, as shown in Fig. 9 (left), which is not negligible compared to the relative statistical uncertainty on the signal yield (shown in Fig. 2, bottom). These two uncertainties are compared in Fig. 9 (right). The systematic uncertainty related to the random picking efficiency reaches up to 20% of the statistical uncertainty in these pseudoexperiments. It was already shown in Fig. 2 that the statistical uncertainty of the randomly picked sample is larger than that of the sample with all candidates. The systematic uncertainty is an additional penalty.

Absolute efficiencies are difficult to determine at hadron colliders and thus potentially involve large systematic uncertainties. It is therefore common practice to measure relative branching fractions or cross-sections by normalising the signal to a well-known high-yield normalisation mode [8, 74, 76, 120, 121]. In this case, the ratio of candidate removal efficiencies for the signal and normalisation modes matters. These efficiencies do not only depend on the signal and calibration modes, but also on their respective backgrounds. If the rate of companion candidates, as well as their properties, are not identical for both modes (which is likely), a systematic uncertainty must be determined. In order to profit from the statistical power of the larger calibration sample, analysts should demonstrate that the behaviour of companion candidates is the same for the signal and the calibration mode. Otherwise, the systematic uncertainty described above applies.

4 Recommendations

In the following recommendations are given.

1. Analysts should report the candidate multiplicity and to which category the candidates belong (see in Section 2). It should be specified if they contribute to (and potentially bias) the signal component or only to the background.

2. The handling of multiple candidates should be performed after the full selection has been applied.
3. Analysts should study the available techniques and select that which minimises the biases and the total uncertainty.
4. Not doing anything usually avoids biases at the price of a slightly higher background level. The effect on the statistical uncertainty is usually negligible. In presence of many events with overlapping candidates, the uncertainty coverage should be checked using pseudoexperiments.
5. If overlaps with signal are present, it should be checked whether they behave signal- or background-like. If neither, a dedicated fit component is required to avoid biases.
6. A candidate-removal technique is a selection requirement. It has an associated signal efficiency which should be reported.
7. Any candidate-removal technique can cause biases which need to be studied and may require a correction. Differences between the signal and simulation or a control samples should be assessed and a systematic uncertainty assigned.
8. In case of arbitration using a best-candidate selection, additional biases can be due to the choice of the discriminating variable. This technique is discouraged.
9. If arbitration is nevertheless chosen, analysts should demonstrate that it improves the precision of the measurement and assign a systematic uncertainty.
10. The most important recommendation is that analysts should have a strategy and describe it in the publication. If there is a possibility for any bias a systematic uncertainty should be assessed.

5 Conclusion

This paper shows that the presence of multiple candidates can cause biases in measurements of rates, asymmetries or particle properties which are much larger than the statistical precision. These biases may be difficult to estimate using simulation or control samples.

In most cases the least biasing technique is to keep all candidates, at the price of a slightly higher statistical uncertainty. It is recommended not to select a single best candidate per event, as this procedure may generate biases.

In publications analysts should report the rate and nature of multiple candidates, outline the strategy how to deal with them and assess systematic uncertainties. Detailed recommendations are given in Sec. 4.

Acknowledgements

The author thanks I. Belyaev, U. Egede, V. Gligorov, N. de Groot, T. du Pree, T. Gershon, D. Martínez Santos, G. Raven, T. Ruf, P. Seyfert, S. Stahl, S. Stone, N. Tuning and I. van Vulpen for useful discussions. In particular M. Merk, L. Dufour, and W. Hulsbergen are thanked for carefully reading the manuscript.

This work is part of the NWO Institute Organisation (NWO-I), which is financed by the Netherlands Organisation for Scientific Research (NWO).

References

- [1] LHCb collaboration, R. Aaij *et al.*, *Observation of CP violation in charm decays*, Phys. Rev. Lett. **122** (2019) 211803, arXiv:1903.08726.
- [2] LHCb collaboration, *Framework TDR for the LHCb Upgrade: Technical Design Report*, CERN-LHCC-2012-007, 2012.
- [3] T. Aushev *et al.*, *Physics at Super B Factory*, arXiv:1002.5012.
- [4] HL-LHC, HE-LHC Working Group 1, P. Azzi *et al.*, *Standard Model Physics at the HL-LHC and HE-LHC*, arXiv:1902.04070; HL-LHC, HE-LHC Working Group 2, M. Cepeda *et al.*, *Higgs Physics at the HL-LHC and HE-LHC*, arXiv:1902.00134; A. Cerri *et al.*, *Opportunities in Flavour Physics at the HL-LHC and HE-LHC*, arXiv:1812.07638.
- [5] A. Abada *et al.*, *FCC Physics Opportunities*, Eur. Phys. J. **C79** (2019) 474.
- [6] ATLAS collaboration, G. Aad *et al.*, *Observation of a new particle in the search for the Standard Model Higgs boson with the ATLAS detector at the LHC*, Phys. Lett. **B716** (2012) 1, arXiv:1207.7214.
- [7] CMS collaboration, S. Chatrchyan *et al.*, *Observation of a new boson at a mass of 125 GeV with the CMS experiment at the LHC*, Phys. Lett. **B716** (2012) 30, arXiv:1207.7235.
- [8] LHCb collaboration, R. Aaij *et al.*, *Measurement of the $B_s^0 \rightarrow \mu^+ \mu^-$ branching fraction and effective lifetime and search for $B^0 \rightarrow \mu^+ \mu^-$ decays*, Phys. Rev. Lett. **118** (2017) 191801, arXiv:1703.05747.
- [9] ATLAS collaboration, M. Aaboud *et al.*, *Study of the rare decays of B_s^0 and B^0 into muon pairs from data collected during the LHC Run 1 with the ATLAS detector*, Eur. Phys. J. **C76** (2016) 513, arXiv:1604.04263.
- [10] Internal recommendations exist in LHCb and probably other collaborations. But these are not available for external readers. The present document is based on the LHCb recommendations.
- [11] As an example, the likelihood of multiple signal candidate events can be determined in the case of $D^{*\pm} \rightarrow \bar{D} \pi^\pm$ with $\bar{D} \rightarrow K^+ K^-$ from Ref. [1]. The probability of seeing another signal $D^{*\pm}$ meson in the same event (which thus contains a charm quark pair) is given by the $D^{*\pm}$ hadronisation fraction, multiplied by the branching fractions and the experimental efficiency. Using the $c\bar{c}$ cross-section and hadronisation fractions from Ref. [122], one can infer this probability to be less than 10^{-6} , while the multiple candidate rate is reported as about 10%.

- [12] LHCb collaboration, R. Aaij *et al.*, *Prompt charm production in pp collisions at $\sqrt{s} = 7$ TeV*, Nucl. Phys. **B871** (2013) 1, arXiv:1302.2864.
- [13] This assumption may occasionally be wrong, as shown in conference proceedings which sometimes give more information than the corresponding publication.
- [14] LHCb collaboration, R. Aaij *et al.*, *Evidence for CP violation in time-integrated $D^0 \rightarrow h^- h^+$ decay rates*, Phys. Rev. Lett. **108** (2012) 111602, arXiv:1112.0938.
- [15] ATLAS collaboration, G. Aad *et al.*, *Search for a standard model Higgs boson in the mass range 200-600 GeV in the $H \rightarrow ZZ \rightarrow \ell^+ \ell^- q \bar{q}$ decay channel with the ATLAS detector*, Phys. Lett. **B717** (2012) 70, arXiv:1206.2443.
- [16] LHCb collaboration, R. Aaij *et al.*, *Observation of two new Ξ_b^- baryon resonances*, Phys. Rev. Lett. **114** (2015) 062004, arXiv:1411.4849.
- [17] BaBar collaboration, Lees, J. P. *et al.*, *Search for a light Higgs resonance in radiative decays of the $\Upsilon(1S)$ with a charm tag*, Phys. Rev. **D91** (2015) 071102, arXiv:1502.06019.
- [18] LHCb collaboration, R. Aaij *et al.*, *Measurement of the difference of time-integrated CP asymmetries in $D^0 \rightarrow K^- K^+$ and $D^0 \rightarrow \pi^- \pi^+$ decays*, Phys. Rev. Lett. **116** (2016) 191601, arXiv:1602.03160.
- [19] LHCb collaboration, R. Aaij *et al.*, *Amplitude analysis of $B^- \rightarrow D^+ \pi^- \pi^-$ decays*, Phys. Rev. **D94** (2016) 072001, arXiv:1608.01289.
- [20] LHCb collaboration, R. Aaij *et al.*, *Search for structure in the $B_s^0 \pi^\pm$ invariant mass spectrum*, Phys. Rev. Lett. **117** (2016) 152003, arXiv:1608.00435.
- [21] LHCb collaboration, R. Aaij *et al.*, *Measurement of the b -quark production cross-section in 7 and 13 TeV pp collisions*, Phys. Rev. Lett. **118** (2017) 052002, Erratum *ibid.* **119** (2017) 169901, arXiv:1612.05140.
- [22] LHCb collaboration, R. Aaij *et al.*, *Study of the $D^0 p$ amplitude in $\Lambda_b^0 \rightarrow D^0 p \pi^-$ decays*, JHEP **05** (2017) 030, arXiv:1701.07873.
- [23] LHCb collaboration, R. Aaij *et al.*, *Search for CP violation in $\Lambda_c^+ \rightarrow p K^- K^+$ and $\Lambda_c^+ \rightarrow p \pi^- \pi^+$ decays*, JHEP **03** (2018) 182, arXiv:1712.07051.
- [24] LHCb collaboration, R. Aaij *et al.*, *Observation of the decay $\Lambda_b^0 \rightarrow \Lambda_c^+ p \bar{p} \pi^-$* , Phys. Lett. **B784** (2018) 101, arXiv:1804.09617.
- [25] LHCb collaboration, R. Aaij *et al.*, *Prompt Λ_c^+ production in p Pb collisions at $\sqrt{s_{NN}} = 5.02$ TeV*, JHEP **02** (2019) 102, arXiv:1809.01404.
- [26] LHCb collaboration, R. Aaij *et al.*, *Measurement of the mass and production rate of Ξ_b^- baryons*, Phys. Rev. **D99** (2019) 052006, arXiv:1901.07075.
- [27] CMS collaboration, A. M. Sirunyan *et al.*, *Studies of $B_{s2}^*(5840)^0$ and $B_{s1}(5830)^0$ mesons including the observation of the $B_{s2}^*(5840)^0 \rightarrow B^0 K_S^0$ decay in proton-proton collisions at $\sqrt{s} = 8$ TeV*, Eur. Phys. J. **C78** (2018) 939, arXiv:1809.03578.

- [28] ATLAS collaboration, M. Aaboud *et al.*, *Search for a Structure in the $B_s^0\pi^\pm$ Invariant Mass Spectrum with the ATLAS Experiment*, Phys. Rev. Lett. **120** (2018) 202007, arXiv:1802.01840.
- [29] LHCb collaboration, R. Aaij *et al.*, *Measurement of the CP-violating phase ϕ_s from $B_s^0 \rightarrow J/\psi \pi^+ \pi^-$ decays in 13 TeV pp collisions*, arXiv:1903.05530, submitted to Phys. Lett. B.
- [30] LHCb collaboration, R. Aaij *et al.*, *Updated measurement of time-dependent CP-violating observables in $B_s^0 \rightarrow J/\psi K^+ K^-$ decays*, arXiv:1906.08356, submitted to EPJC.
- [31] D0 collaboration, B. Abbott *et al.*, *Small angle J/ψ production in $p\bar{p}$ collisions at $\sqrt{s} = 1.8$ TeV*, Phys. Rev. Lett. **82** (1999) 35, arXiv:hep-ex/9807029.
- [32] CDF collaboration, D. Acosta *et al.*, *Measurement of the J/ψ meson and b -hadron production cross sections in $p\bar{p}$ collisions at $\sqrt{s} = 1960$ GeV*, Phys. Rev. **D71** (2005) 032001, arXiv:hep-ex/0412071.
- [33] PHENIX collaboration, A. Adare *et al.*, *J/ψ production versus transverse momentum and rapidity in p^+p collisions at $\sqrt{s} = 200$ GeV*, Phys. Rev. Lett. **98** (2007) 232002, arXiv:hep-ex/0611020.
- [34] CMS collaboration, V. Khachatryan *et al.*, *Prompt and non-prompt J/ψ production in pp collisions at $\sqrt{s} = 7$ TeV*, Eur. Phys. J. **C71** (2011) 1575, arXiv:1011.4193.
- [35] LHCb collaboration, R. Aaij *et al.*, *Measurement of J/ψ production in pp collisions at $\sqrt{s} = 7$ TeV*, Eur. Phys. J. **C71** (2011) 1645, arXiv:1103.0423.
- [36] LHCb collaboration, R. Aaij *et al.*, *Observation of J/ψ -pair production in pp collisions at $\sqrt{s} = 7$ TeV*, Phys. Lett. **B707** (2012) 52, arXiv:1109.0963.
- [37] ALICE collaboration, K. Aamodt *et al.*, *Rapidity and transverse momentum dependence of inclusive J/ψ production in pp collisions at $\sqrt{s} = 7$ TeV*, Phys. Lett. **B704** (2011) 442, Erratum *ibid.* **B718** (2012) 692, arXiv:1105.0380.
- [38] ATLAS collaboration, G. Aad *et al.*, *Measurement of the differential cross-sections of inclusive, prompt and non-prompt J/ψ production in proton-proton collisions at $\sqrt{s} = 7$ TeV*, Nucl. Phys. **B850** (2011) 387, arXiv:1104.3038.
- [39] CMS collaboration, S. Chatrchyan *et al.*, *J/ψ and $\psi(2S)$ production in pp collisions at $\sqrt{s} = 7$ TeV*, JHEP **02** (2012) 011, arXiv:1111.1557.
- [40] CMS collaboration, V. Khachatryan *et al.*, *Measurement of prompt J/ψ pair production in pp collisions at $\sqrt{s} = 7$ TeV*, JHEP **09** (2014) 094, arXiv:1406.0484.
- [41] CDF collaboration, T. A. Aaltonen *et al.*, *Study of orbitally excited B mesons and evidence for a new $B\pi$ resonance*, Phys. Rev. **D90** (2014) 012013, arXiv:1309.5961.

- [42] CMS collaboration, V. Khachatryan *et al.*, *Search for Resonant Production of High-Mass Photon Pairs in Proton-Proton Collisions at $\sqrt{s} = 8$ and 13 TeV*, Phys. Rev. Lett. **117** (2016) 051802, arXiv:1606.04093.
- [43] CMS collaboration, V. Khachatryan *et al.*, *Observation of the diphoton decay of the Higgs boson and measurement of its properties*, Eur. Phys. J. **C74** (2014) 3076, arXiv:1407.0558.
- [44] BaBar collaboration, J. P. Lees *et al.*, *Measurement of the inclusive electron spectrum from B meson decays and determination of $|V_{ub}|$* , Phys. Rev. **D95** (2016) 072001, arXiv:1611.05624.
- [45] Belle collaboration, V. Bhardwaj *et al.*, *Inclusive and exclusive measurements of B decays to χ_{c1} and χ_{c2} at Belle*, Phys. Rev. D **93** (2016) 052016, arXiv:1512.02672.
- [46] LHCb collaboration, R. Aaij *et al.*, *B flavour tagging using charm decays at the LHCb experiment*, JINST **10** (2015) P10005, arXiv:1507.07892.
- [47] LHCb collaboration, R. Aaij *et al.*, *Observation of CP violation in $B^\pm \rightarrow DK^\pm$ decays*, Phys. Lett. **B712** (2012) 203, Erratum *ibid.* **B713** (2012) 351, arXiv:1203.3662.
- [48] LHCb collaboration, R. Aaij *et al.*, *Observation of the decay $B_s^0 \rightarrow \bar{D}^{*0} \phi$ and search for the mode $B^0 \rightarrow \bar{D}^0 \phi$* , Phys. Rev. **D98** (2018) 071103(R), arXiv:1807.01892.
- [49] LHCb collaboration, R. Aaij *et al.*, *Measurement of CP observables in $B^\pm \rightarrow D^{(*)}K^\pm$ and $B^\pm \rightarrow D^{(*)}\pi^\pm$ decays*, Phys. Lett. **B777** (2017) 16, arXiv:1708.06370.
- [50] BES III collaboration, M. Ablikim *et al.*, *Confirmation of a charged charmoniumlike state $Z_c(3885)^\mp$ in $e^+e^- \rightarrow \pi^\pm(D\bar{D}^*)^\mp$ with double D tag*, Phys. Rev. **D92** (2015) 092006, arXiv:1509.01398.
- [51] LHCb collaboration, R. Aaij *et al.*, *Measurements of the B^+ , B^0 , B_s^0 meson and Λ_b^0 baryon lifetimes*, JHEP **04** (2014) 114, arXiv:1402.2554.
- [52] Belle collaboration, S. Sandilya *et al.*, *Search for Bottomonium States in Exclusive Radiative $\Upsilon(2S)$ Decays*, Phys. Rev. Lett. **111** (2013) 112001, arXiv:1306.6212.
- [53] DELPHI collaboration, J. Abdallah *et al.*, *Determination of heavy quark non-perturbative parameters from spectral moments in semileptonic B decays*, Eur. Phys. J. **C45** (2006) 35, arXiv:hep-ex/0510024.
- [54] DELPHI collaboration, J. Abdallah *et al.*, *Measurement of $|V_{cb}|$ using the semileptonic decay $B^0 \rightarrow D^{*+}\ell^-\bar{\nu}_\ell$* , Eur. Phys. J. **C33** (2004) 213, arXiv:hep-ex/0401023.
- [55] ALEPH collaboration, R. Barate *et al.*, *The Forward - backward asymmetry for charm quarks at the Z*, Phys. Lett. **B434** (1998) 415, arXiv:hep-ex/9811015.

- [56] Belle collaboration, J. Schumann *et al.*, *Observation of $\bar{B}^0 \rightarrow D^0 \eta'$ and $\bar{B}^0 \rightarrow D^{*0} \eta'$* , Phys. Rev. **D72** (2005) 011103, arXiv:hep-ex/0501013.
- [57] Belle collaboration, S. Nishida *et al.*, *Observation of $B^+ \rightarrow K^+ \eta \gamma$* , Phys. Lett. **B610** (2005) 23, arXiv:hep-ex/0411065.
- [58] ATLAS collaboration, M. Aaboud *et al.*, *Search for squarks and gluinos in events with hadronically decaying tau leptons, jets and missing transverse momentum in proton-proton collisions at $\sqrt{s} = 13$ TeV recorded with the ATLAS detector*, Eur. Phys. J. **C76** (2016) 683, arXiv:1607.05979.
- [59] CMS collaboration, V. Khachatryan *et al.*, *Angular analysis of the decay $B^0 \rightarrow K^{*0} \mu^+ \mu^-$ from pp collisions at $\sqrt{s} = 8$ TeV*, Phys. Lett. **B753** (2016) 424, arXiv:1507.08126.
- [60] CMS collaboration, S. Chatrchyan *et al.*, *Measurement of the properties of a Higgs boson in the four-lepton final state*, Phys. Rev. **D89** (2014) 092007, arXiv:1312.5353.
- [61] ATLAS collaboration, G. Aad *et al.*, *Measurement of the Higgs boson mass from the $H \rightarrow \gamma \gamma$ and $H \rightarrow ZZ^* \rightarrow 4\ell$ channels with the ATLAS detector using 25 fb⁻¹ of pp collision data*, Phys. Rev. **D90** (2014) 052004, arXiv:1406.3827.
- [62] ATLAS, M. Aaboud *et al.*, *Angular analysis of $B_d^0 \rightarrow K^{*0} \mu^+ \mu^-$ decays in pp collisions at $\sqrt{s} = 8$ TeV with the ATLAS detector*, JHEP **10** (2018) 047, arXiv:1805.04000.
- [63] LHCb collaboration, R. Aaij *et al.*, *Observation of the decay $B_s^0 \rightarrow \bar{D}^0 K^+ K^-$* , Phys. Rev. **D98** (2018) 072006, arXiv:1807.01891.
- [64] LHCb collaboration, R. Aaij *et al.*, *Study of the $B^0 \rightarrow \rho(770)^0 K^{*0}(892)^0$ decay with an amplitude analysis of $B^0 \rightarrow (\pi^+ \pi^-)(K^+ \pi^-)$ decays*, JHEP **05** (2019) 026, arXiv:1812.07008.
- [65] Belle and BaBar collaborations, A. J. Bevan *et al.*, *The Physics of the B Factories*, Eur. Phys. J. **C74** (2014) 3026, arXiv:1406.6311.
- [66] BaBar collaboration, B. Aubert *et al.*, *Measurement of the branching fractions for the exclusive decays of B^0 and B^+ to $\bar{D}^{(*)} D^{(*)} K$* , Phys. Rev. **D68** (2003) 092001, arXiv:hep-ex/0305003.
- [67] BaBar collaboration, J. P. Lees *et al.*, *Study of $B^{\pm,0} \rightarrow J/\psi K^+ K^- K^{\pm,0}$ and search for $B^0 \rightarrow J/\psi \phi$ at BABAR*, Phys. Rev. **D91** (2015) 012003, arXiv:1407.7244.
- [68] Belle collaboration, A. Ishikawa *et al.*, *Measurement of Forward-Backward Asymmetry and Wilson Coefficients in $B \rightarrow K^* \ell^+ \ell^-$* , Phys. Rev. Lett. **96** (2006) 251801, arXiv:hep-ex/0603018.
- [69] BES III collaboration, M. Ablikim *et al.*, *Measurement of y_{CP} in $D^0 - \bar{D}^0$ oscillation using quantum correlations in $e^+ e^- \rightarrow D^0 \bar{D}^0$ at $\sqrt{s} = 3.773$ GeV*, Phys. Lett. **B744** (2015) 339, arXiv:1501.01378.

- [70] CLEO collaboration, N. E. Adam *et al.*, *A Study of Exclusive Charmless Semileptonic B Decay and $|V_{ub}|$* , Phys. Rev. Lett. **99** (2007) 041802, arXiv:hep-ex/0703041.
- [71] Belle collaboration, S.-K. Choi *et al.*, *Measurements of $B \rightarrow \bar{D}D_{s0}^{*+}(2317)$ decay rates and a search for isospin partners of the $D_{s0}^{*+}(2317)$* , Phys. Rev. **D91** (2015) 092011, Addendum *ibid.* **D92** (2015) 039905, arXiv:1504.02637.
- [72] A candidate arbitration is sometimes part of the design of the selection. For instance the highest p_T lepton, or the most energetic jet may be used as seed to further reconstruction. between data and simulation, or signal and control channels, such cases. More generally, the particle trajectory reconstruction software — known as pattern recognition — applies arbitration by design [123]. The pattern recognition decides which detector signal ("hit") to add to the trajectory of a particle based its the extrapolation to the detector. The closest hit is usually selected. The tracking efficiency is calibrated using data [124–126], thus removing potential biases.
- [73] In many analyses the correct determination of the creation point of the particle of interest is equally important as identifying the signal. Examples are measurements of decay-time dependent observables, or analyses of candidates which do not allow the determination of a decay vertex as diphotons. At colliders the origin is usually the primary vertex, for which ambiguities remaining after the selection are addressed by arbitration [9, 38, 127–136] or random picking [74–76, 78, 137]. Wrong assignments should be accounted for by a resolution function or by an additional background contribution.
- [74] LHCb collaboration, R. Aaij *et al.*, *Measurement of the $B_s^0 \rightarrow J/\psi K_S^0$ branching fraction*, Phys. Lett. **B713** (2012) 172, arXiv:1205.0934.
- [75] LHCb collaboration, R. Aaij *et al.*, *Measurement of the effective $B_s^0 \rightarrow J/\psi K_S^0$ lifetime*, Nucl. Phys. **B873** (2013) 275, arXiv:1304.4500.
- [76] LHCb collaboration, R. Aaij *et al.*, *Observation of the $\Lambda_b^0 \rightarrow J/\psi p\pi^-$ decay*, JHEP **07** (2014) 103, arXiv:1406.0755.
- [77] ATLAS collaboration, G. Aad *et al.*, *Searches for heavy long-lived charged particles with the ATLAS detector in proton-proton collisions at $\sqrt{s} = 8$ TeV*, JHEP **01** (2015) 068, arXiv:1411.6795.
- [78] LHCb collaboration, R. Aaij *et al.*, *Measurement of the time-dependent CP asymmetries in $B_s^0 \rightarrow J/\psi K_S^0$* , JHEP **06** (2015) 131, arXiv:1503.07055.
- [79] LHCb collaboration, R. Aaij *et al.*, *Observation of $B_s^0 \rightarrow \bar{D}^0 K_S^0$ and evidence for $B_s^0 \rightarrow \bar{D}^{*0} K_S^0$ decays*, Phys. Rev. Lett. **116** (2016) 161802, arXiv:1603.02408.
- [80] LHCb collaboration, R. Aaij *et al.*, *Measurement of the $B_s^0 \rightarrow J/\psi \eta$ lifetime*, Phys. Lett. **B762** (2016) 484, arXiv:1607.06314.
- [81] LHCb collaboration, R. Aaij *et al.*, *Measurement of matter-antimatter differences in beauty baryon decays*, Nature Physics **13** (2017) 391, arXiv:1609.05216.

- [82] LHCb collaboration, R. Aaij *et al.*, *Measurement of CP asymmetry in $D^0 \rightarrow K^+ K^-$ decays*, Phys. Lett. **B767** (2017) 177, arXiv:1610.09476.
- [83] LHCb collaboration, R. Aaij *et al.*, *Measurement of the J/ψ pair production cross-section in pp collisions at $\sqrt{s} = 13$ TeV*, JHEP **06** (2017) 047, Erratum ibid. **10** (2017) 068, arXiv:1612.07451.
- [84] LHCb collaboration, R. Aaij *et al.*, *Test of lepton universality with $B^0 \rightarrow K^{*0} \ell^+ \ell^-$ decays*, JHEP **08** (2017) 055, arXiv:1705.05802.
- [85] LHCb collaboration, R. Aaij *et al.*, *Observation of the doubly charmed baryon Ξ_{cc}^{++}* , Phys. Rev. Lett. **119** (2017) 112001, arXiv:1707.01621.
- [86] LHCb collaboration, R. Aaij *et al.*, *Measurement of CP violation in $B^0 \rightarrow J/\psi K_S^0$ and $B^0 \rightarrow \psi(2S) K_S^0$ decays*, JHEP **11** (2017) 170, arXiv:1709.03944.
- [87] LHCb collaboration, R. Aaij *et al.*, *Measurement of the ratio of branching fractions of the decays $\Lambda_b^0 \rightarrow \psi(2S) \Lambda$ and $\Lambda_b^0 \rightarrow J/\psi \Lambda$* , JHEP **03** (2019) 126, arXiv:1902.02092.
- [88] LHCb collaboration, R. Aaij *et al.*, *First measurement of the CP-violating phase $\phi_s^{d\bar{d}}$ in $B_s^0 \rightarrow (K^+ \pi^-)(K^- \pi^+)$ decays*, JHEP **03** (2018) 140, arXiv:1712.08683.
- [89] LHCb collaboration, R. Aaij *et al.*, *Search for CP violation using triple product asymmetries in $\Lambda_b^0 \rightarrow p K^- \pi^+ \pi^-$, $\Lambda_b^0 \rightarrow p K^- K^+ K^-$, and $\Xi_b^0 \rightarrow p K^- K^- \pi^+$ decays*, JHEP **08** (2018) 039, arXiv:1805.03941.
- [90] LHCb collaboration, R. Aaij *et al.*, *Search for CP violation in $\Lambda_b^0 \rightarrow p K^-$ and $\Lambda_b^0 \rightarrow p \pi^-$ decays*, Phys. Lett. **B784** (2018) 101, arXiv:1807.06544.
- [91] LHCb collaboration, R. Aaij *et al.*, *Measurement of CP asymmetries in two-body $B_{(s)}^0$ -meson decays to charged pions and kaons*, Phys. Rev. **D98** (2018) 032004, arXiv:1805.06759.
- [92] LHCb collaboration, R. Aaij *et al.*, *Measurement of angular and CP asymmetries in $D^0 \rightarrow \pi^+ \pi^- \mu^+ \mu^-$ and $D^0 \rightarrow K^+ K^- \mu^+ \mu^-$ decays*, Phys. Rev. Lett. **121** (2018) 091801, arXiv:1806.10793.
- [93] CLEO collaboration, M. Artuso *et al.*, *Search for the decay $\bar{B}^0 \rightarrow D^{*0} \gamma$* , Phys. Rev. Lett. **84** (2000) 4292, arXiv:hep-ex/0001002.
- [94] CLEO collaboration, G. S. Adams *et al.*, *Amplitude analyses of the decays $\chi_{c1} \rightarrow \eta \pi^+ \pi^-$ and $\chi_{c1} \rightarrow \eta' \pi^+ \pi^-$* , Phys. Rev. **D84** (2011) 112009, arXiv:1109.5843.
- [95] ATLAS collaboration, G. Aad *et al.*, *Measurement of the inclusive W^\pm and Z/γ^* cross sections in the electron and muon decay channels in pp collisions at $\sqrt{s} = 7$ TeV with the ATLAS detector*, Phys. Rev. **D85** (2012) 072004, arXiv:1109.5141.
- [96] LHCb collaboration, R. Aaij *et al.*, *Measurement of forward W and Z boson production in pp collisions at $\sqrt{s} = 8$ TeV*, JHEP **01** (2016) 155, arXiv:1511.08039.

- [97] COMPASS collaboration, M. Aghasyan *et al.*, *Observation of $X(3872)$ muoproduction at COMPASS*, Phys. Lett. **B783** (2018) 334, arXiv:1707.01796.
- [98] LHCb collaboration, R. Aaij *et al.*, *Measurement of the branching fraction and CP asymmetry in $B^+ \rightarrow J/\psi \rho^+$ decays*, Eur. Phys. J. **C79** (2019) 537, arXiv:1812.07041.
- [99] An exponential shape would be more physical, but would be an unnecessary complication of the model.
- [100] In the general case one would expect a different mass distribution for overlapping candidates. This different distribution could then be taken into account in the fit. The author is not aware of any publication where this was done. Therefore it is assumed here that overlaps behave background-like.
- [101] For example a $B^0 \rightarrow J/\psi K^{*0}$ signal decay with $J/\psi \rightarrow \mu^+ \mu^-$ and $K^{*0} \rightarrow K^+ \pi^-$ could have a companion $\bar{B}^0 \rightarrow J/\psi \bar{K}^{*0}$ candidate which shares the same J/ψ but adds an unrelated $\bar{K}^{*0} \rightarrow K^- \pi^+$ candidate. Such a situation produces a correlation between the B^0 signal yield and the \bar{B}^0 background yield.
- [102] Weighting leads to the same results as the random selection provided the weights are properly taken into account in the fit. Event removal is equivalent to random picking with probability 0 instead of $1/2$. The resulting biases have twice the size of those obtained with this method.
- [103] Mathematical expressions can be found in the ancillary material at <https://arxiv.org/src/1703.01128/anc/Ancillary.pdf>.
- [104] Variation of the probability of a background candidate to have a companion is tested with $\mathcal{P}_{\text{sig}}^{B^0} = \mathcal{P}_{\text{sig}}^{\bar{B}^0} = 0$. When taking all candidates, the effect of larger $\mathcal{P}_{\text{bkg}}^{B^0}$ and $\mathcal{P}_{\text{bkg}}^{\bar{B}^0}$ values is to increase the background level, which does not bias any measurement but degrades the uncertainty in the same way as $\mathcal{P}_{\text{sig}}^{B^0}$ and $\mathcal{P}_{\text{sig}}^{\bar{B}^0}$ do. However, when a candidate selection technique is applied, only background candidates get removed resulting in a situation equivalent to the clean case.
- [105] This systematic uncertainty may be negligible and thus not be reported.
- [106] In the decay $B^+ \rightarrow D^+ \pi^0$ companion candidates can be generated starting from the signal D^+ and adding a fake π^0 . By construction, the two candidates have the same flavour and the swapping probabilities are zero. In the decay $B^+ \rightarrow D_{CP} \mu^+ \nu$ where D_{CP} is a D^0 meson decaying to a CP eigenstate, if a true D_{CP} is combined with a muon from the other B , the latter is likely to be of the opposite flavour and hence the flavours of signal and overlapping candidate are anti-correlated. The swapping probabilities are close to unity. For the decay $B^0 \rightarrow J/\psi K^{*0}$ [101], the flavour of the fake B^0 candidate depends on the K^{*0} to \bar{K}^{*0} production ratio, which may be slightly (anti-)correlated with that of B^0 versus \bar{B}^0 , $\mathcal{P}_{\text{swap}}^{\text{sig } B^0} \simeq \mathcal{P}_{\text{swap}}^{\text{sig } \bar{B}^0} \simeq 0.5$.
- [107] Such situations are not necessarily desirable, as these probabilities may not be reproduced well in the simulation or in a control sample, leading to incorrect efficiency corrections.

- [108] It is common for B background candidates to be formed from a combination of final-state particles from different b hadrons, resulting in a visible lifetime that is lower than that of a true b hadron. In the case of overlaps, some components of the candidate are from the true signal, resulting in a visible lifetime which is larger than that of background but lower than τ_{B^0} . In reality the actual factors may differ considerably from the values $1/2$ and $1/3$ used here and the distributions would not be pure exponential functions. However, the conclusions are not affected as long as the distributions are smooth curves.
- [109] This resolution function is irrelevant for this study, but helps making the fit more stable.
- [110] M. Pivk and F. R. Le Diberder, *sPlot: A statistical tool to unfold data distributions*, Nucl. Instrum. Meth. **A555** (2005) 356, arXiv:physics/0402083.
- [111] Y. Xie, *sFit: a method for background subtraction in maximum likelihood fit*, arXiv:0905.0724.
- [112] The situation may be very different if the overlaps are peaking in mass.
- [113] LHCb collaboration, R. Aaij *et al.*, *Measurement of CP asymmetry in $B_s^0 \rightarrow D_s^\mp K^\pm$ decays*, JHEP **11** (2014) 060, arXiv:1407.6127.
- [114] K. De Bruyn *et al.*, *Branching Ratio Measurements of B_s Decays*, Phys. Rev. **D86** (2012) 014027, arXiv:1204.1735.
- [115] This risk has been recognised by the CMS collaboration in the analysis of Higgs bosons decaying to four leptons [60] used in the Higgs boson mass measurement [116]. It is reported that the used arbitration procedure based on dilepton masses does not sculpt the background shape. The arbitration procedure applied by the ATLAS collaboration is different and there is no statement on potential biases [61].
- [116] ATLAS and CMS collaborations, G. Aad *et al.*, *Combined Measurement of the Higgs Boson Mass in pp Collisions at $\sqrt{s} = 7$ and 8 TeV with the ATLAS and CMS Experiments*, Phys. Rev. Lett. **114** (2015) 191803, arXiv:1503.07589.
- [117] CMS collaboration, V. Khachatryan *et al.*, *Charged particle multiplicities in pp interactions at $\sqrt{s} = 0.9, 2.36,$ and 7 TeV*, JHEP **01** (2011) 079, arXiv:1011.5531.
- [118] LHCb collaboration, R. Aaij *et al.*, *Measurement of charged particle multiplicities and densities in pp collisions at $\sqrt{s} = 7$ TeV in the forward region*, Eur. Phys. J. **C74** (2014) 2888, arXiv:1402.4430.
- [119] This may not be true in the general case. If the mass distribution of companion candidates and of the background are different, the sPlot technique [110] may not be able to disentangle all species correctly, unless all these distributions are known.
- [120] CMS collaboration, S. Chatrchyan *et al.*, *Angular analysis and branching fraction measurement of the decay $B^0 \rightarrow K^{*0} \mu^+ \mu^-$* , Phys. Lett. **B727** (2013) 77, arXiv:1308.3409.

- [121] LHCb collaboration, R. Aaij *et al.*, *Measurement of the S-wave fraction in $B^0 \rightarrow K^+\pi^-\mu^+\mu^-$ decays and the $B^0 \rightarrow K^*(892)^0\mu^+\mu^-$ differential branching fraction*, JHEP **11** (2016) 047, Erratum *ibid.* **04** (2017) 142, arXiv:1606.04731.
- [122] LHCb collaboration, R. Aaij *et al.*, *Measurements of prompt charm production cross-sections in pp collisions at $\sqrt{s} = 13$ TeV*, JHEP **03** (2016) 159, Erratum *ibid.* **09** (2016) 013, Erratum *ibid.* **05** (2017) 074, arXiv:1510.01707.
- [123] R. Frühwirth, *Application of Kalman filtering to track and vertex fitting*, Nucl. Instrum. Meth. **A262** (1987) 444.
- [124] ATLAS collaboration, *Performance of the ATLAS Inner Detector Track and Vertex Reconstruction in the High Pile-Up LHC Environment*, Tech. Rep. ATLAS-CONF-2012-042, CERN, Geneva, 2012.
- [125] CMS collaboration, S. Chatrchyan *et al.*, *Description and performance of track and primary-vertex reconstruction with the CMS tracker*, JINST **9** (2014) P10009, arXiv:1405.6569.
- [126] LHCb collaboration, R. Aaij *et al.*, *Measurement of the track reconstruction efficiency at LHCb*, JINST **10** (2015) P02007, arXiv:1408.1251.
- [127] ATLAS collaboration, G. Aad *et al.*, *Search for displaced vertices arising from decays of new heavy particles in 7 TeV pp collisions at ATLAS*, Phys. Lett. **B707** (2012) 478, arXiv:1109.2242.
- [128] ATLAS collaboration, G. Aad *et al.*, *Search for strong gravity signatures in same-sign dimuon final states using the ATLAS detector at the LHC*, Phys. Lett. **B709** (2012) 322, arXiv:1111.0080.
- [129] R. Aaij *et al.*, *The LHCb trigger and its performance in 2011*, JINST **8** (2013) P04022, arXiv:1211.3055.
- [130] LHCb collaboration, R. Aaij *et al.*, *First measurement of time-dependent CP violation in $B_s^0 \rightarrow K^+K^-$ decays*, JHEP **10** (2013) 183, arXiv:1308.1428.
- [131] LHCb collaboration, R. Aaij *et al.*, *Study of the kinematic dependences of Λ_b^0 production in pp collisions and a measurement of the $\Lambda_b^0 \rightarrow \Lambda_c^+\pi^-$ branching fraction*, JHEP **08** (2014) 143, arXiv:1405.6842.
- [132] LHCb collaboration, R. Aaij *et al.*, *Measurement of CP violation in $B_s^0 \rightarrow \phi\phi$ decays*, Phys. Rev. **D90** (2014) 052011, arXiv:1407.2222.
- [133] LHCb collaboration, R. Aaij *et al.*, *Precision measurement of CP violation in $B_s^0 \rightarrow J/\psi K^+K^-$ decays*, Phys. Rev. Lett. **114** (2015) 041801, arXiv:1411.3104.
- [134] ATLAS collaboration, G. Aad *et al.*, *Search for direct production of charginos, neutralinos and sleptons in final states with two leptons and missing transverse momentum in pp collisions at $\sqrt{s} = 8$ TeV with the ATLAS detector*, JHEP **05** (2014) 071, arXiv:1403.5294.

- [135] ATLAS collaboration, G. Aad *et al.*, *Search for the direct production of charginos, neutralinos and staus in final states with at least two hadronically decaying taus and missing transverse momentum in pp collisions at $\sqrt{s} = 8$ TeV with the ATLAS detector*, JHEP **10** (2014) 096, arXiv:1407.0350.
- [136] LHCb collaboration, R. Aaij *et al.*, *Measurement of forward J/ψ production cross-sections in pp collisions at $\sqrt{s} = 13$ TeV*, JHEP **10** (2015) 172, Erratum *ibid.* **05** (2017) 063, arXiv:1509.00771.
- [137] LHCb collaboration, R. Aaij *et al.*, *Measurement of CP violation in $B^0 \rightarrow J/\psi K_S^0$ decays*, Phys. Rev. Lett. **115** (2015) 031601, arXiv:1503.07089.